MOLEKUL
eISSN: 2503-0310

Articles
https://doi.org/10.20884/1.jm.2023.18.2.8186

Synthesis and Characterization of 4-amino-*N*'-[(1*E*)-1-(2-hydroxy-6-methyl-4-oxo-4*H*-pyran -3-yl)ethylidene]benzohydrazide and its Cu(II), Ni(II), Zn(II) and Mn(II) Complexes.

Chigozie John Onyinye Anarado[1]*, Chinasa Grace Iziga[1], Collins Ugochukwu Ibeji[2], Ilknur Babahan-Bircan [3], Burak Coban[4], Füsun Cömert [5], Charity Ebere Anarado[1]

[1]Department of Pure and Industrial Chemistry, Faculty of Physical Sciences, Nnamdi Azikiwe University, Awka 420110, Anambra State, Nigeria.
[2]Department of Pure and Industrial Chemistry, Faculty of Physical Sciences, University of Nigeria, Nsukka 410001, Enugu State, Nigeria.
[3]Department of Chemistry, Adnan Menderes University, Aydin, Turkey 09010.
[4]Department of Chemistry, Faculty of Arts and Sciences, ZonguldakBulentEcevit University, Zonguldak 67100, Turkey.
[5]Department of Microbiology, Faculty of Medicine, ZonguldakBulentEcevit University, Zonguldak 67100, Turkey.

*Corresponding author email: cjo.anarado@unizik.edu.ng

Received March 08, 2023; **Accepted** May 31, 2023; **Available online** July 20, 2023

ABSTRACT. New benzohydrazone compound, 4-amino-*N*'-[(1*E*)-1-(2-hydroxy-6-methyl-4-oxo-4*H*-pyran-3-yl)ethylidene] benzohydrazide (HL_1) and its Cu(II), Ni(II), Zn(II) and Mn(II) complexes were synthesized. The structures of HL_1 and its complexes were elucidated by elemental analysis and IR, UV-Vis, ^1H and ^{13}C NMR spectroscopy and mass spectrometry. The infrared spectral data of the complexes revealed that HL_1 coordinated with the metal ions through azomethine nitrogen, enolic oxygen and amide carbonyl oxygen atoms, hence, HL_1 behaves as a monobasic tridentate ligand. UV-Vis data revealed that Zn(II) and Mn(II) complexes adopted octahedral geometry, while Cu(II) and Ni(II) complexes had five-coordinate and square-planar geometries respectively. The mass spectra data and elemental analysis values are in accordance with the calculated values for the suggested molecular formula of the complexes, a confirmation of the 1:1 ligand to metal stoichiometry in case of Cu(II) complex and 2:1 ligands to metal stoichiometry in case of the other complexes.

Keywords: Dehydroacetic acid, Benzohydrazone, Metal complexes

INTRODUCTION

Hydrazones are a class of organic compounds which are characterized by the presence of azomethine (-NH-N=CH-) functional group which plays a major role in the biological activities of the hydrazones (Dutkiewiez et al., 2011; Shakdofa et al., 2014; Asif & Husain, 2013). These compounds demonstrate captivating biological and pharmacological properties such as anticancer, anti-inflammatory, anticonvulsant, antimycobacterial, antiviral, antiplatelet, antitumour, antimicrobial, antidiabetic, antimalarial, etc (Asif & Husain, 2013; Kumar, 2018; Kajal et al., 2014; Kumar et al., 2016; Asyikin et al., 2017). Hydrazones can form a variety of stable complexes with transition and inner transition metals due to their facile keto-enol tautomerization and the availability of other donor sites (Kurup et al., 2010). A literature survey reveals that many synthetic hydrazones incorporating heterocyclic rings are physiologically active (Oukacha-Hikem et al., 2016). 3-acetyl-4-hydroxy-6-methyl-2*H*-pyran-2-one (dehydro acetic acid or DHA) is one such heterocyclic compounds which has proven its significance due to its interesting biological properties. It is a useful starting material for the synthesis of different heterocycles (Fadda & Elattar, 2015; Baldwin *et al.*, 2017; Ullah et al., 2012; Munde et al., 2010). Due to the excellent chelating properties, DHA and its derivatives form various metal complexes that are known to possess antibacterial and antifungal effects (Ullah *et al.*, 2012; Munde et al., 2010; Pal et al., 2014; Gupta *et al.*, 2015; Al Kubaisi & Ismail *et al.*, 1994; Devi et al., 2016). In food technology, DHA is used to enhance vitamin C stability and serves as a preservative in fish sausages (Benosmane et al., 2016; Al Alousi *et al.*, 2008; Kashar & El-Sehli, 2013).

On the other hand, there is a growing interest in benzo hydrazides and their coordination compounds due to their physiological activities as DNA-cleaving agent (Okagu et al., 2019), bactericides and fungicides (Mangamamba et al., 2014) [22], antioxidant (Sherine & Veeramanikandan, 2017; Liu

et al., 2012), anti-inflammatory and anticancer (Kendur et al., 2018). Cu(II) complexes derived from 4-hydroxybenzohydrazide exhibit potential nuclease and antibacterial activities against four pathogenic strains of bacteria; *B. subtilis, P. syringae, P. aeurginosa and S. aureus* (Pal *et al.,* 2014). A series of benzohydrazide derivatives obtained from 1-chloro-3,4-dihydronaphthalene-2-carbaldehyde showed a great cytotoxicity towards prostate cancer cell lines (PC-3, LNCaP) (Arjun *et al.,* 2018). The two combined moieties – the dehydroacetic acid and functionalized benzohydrazide would exhibit synergistic biological activities. Thus, the study of the synthesis and structures of benzohydrazones are important for new drug development. Herein, we report the synthesis and characterization of a novel benzohydrazone and it Cu(II), Ni(II), Zn(II) and Mn(II) complexes.

EXPERIMENTAL SECTION

Materials

The chemicals 4-aminobenzohydrazide and sodium bicarbonate were bought from Sigma-Aldrich. Zinc chloride and nickel(II) chloride hexahydrate were purchased from Guangdong Guanghua Sci-Tech Co. Ltd. Copper(II) chloride dihydrate and manganese(II) chloride tetrahydrate were products of SCP. Dehydroacetic acid was purchased from Merck. These chemicals were used as received. Solvents methanol and DMSO were used without further purification.

Physical Methods

Infrared (IR) spectral data of the compounds were recorded on a Varian 600-IR series spectrometer (Varian Inc., USA) in the 4000 – 400 cm^{-1} range using KBr disc. The ^{1}H and ^{13}C NMR spectra were recorded using Bruker Avance III HD 400 spectrometer (Bruker Corporation, USA) operating at 400 MHz in DMSO-d_6 with TMS as an internal standard. The elemental analysis to determine the C, H, N, and S compositions of the compounds was carried out with Leco/TruSpec Micro Analytical Instrument (IR Technology Services Pvt. Ltd, Navi Mumbai, India). The electronic spectra were recorded using Pye-Unicam in DMSO as a solvent. The mass spectra were recorded with Thermo Fisher TSQ 9000 Triple Quadruple GC-MS/MS (Thermo Fisher Scientific, USA) in positive ion mode using pneumatically assisted electrospray ionization.

Synthesis of 4-amino-N'-[(1E)-1-(2-hydroxy-6-methyl-4-oxo-4H-pyran-3-yl)ethylidene]benzohydrazide (HL_1)

Dehydroacetic acid (4450mg, 26.46 mmol) was dissolved in methanol (30 mL) and reacted with an equivalent of 4-aminobenzohydrazide (4000 mg, 26.46 mmol) using sodium bicarbonate (2220 mg, 26.46 mmol) as a catalyst. The reaction mixture was subsequently refluxed for 1 h. The resulting precipitate (**Figure 1**) was allowed to cool, washed with methanol (10 x 2 mL), air-dried, and stored under silica gel in a vacuum.

Synthesis of Metal complexes

The metal complexes were prepared by reacting the 1:1 stoichiometric ratio of the ligand and Cu(II) salt and the 2:1 stoichiometric ratio of the ligand and Ni(II), Zn(II), and Mn(II) salts (**Figure 2**). A methanolic solution of the respective metal salts $CuCl_2{\cdot}2H_2O$ (570 mg, 3.32 mmol), $NiCl_2{\cdot}6H_2O$ (390 mg, 1.66 mmol), $ZnCl_2$ (230 mg, 1.66 mmol), and $MnCl_2{\cdot}4H_2O$ (330 mg, 1.66 mmol) was added to a stirring methanolic solution of the hydrazone (1000 mg, 3.32mmol). The reaction mixture was refluxed for 2 h. The precipitated solids (fern green, sea green, cream, and yellow, for Cu(II), Ni(II), Zn(II), and Mn(II), respectively) were gravity filtered, washed with methanol (2 x 10 mL) and kept in a desiccator under vacuum.

RESULTS AND DISCUSSION

General Synthesis

The reaction of 3-acetyl-2-hydroxy-6-methyl-4*H*-pyran-4-one with 4-aminobenzohydrazide in the molar ratio of 1:1 in a methanolic medium gave the ligand HL_1 (See the carbon atom numbering in **Figure 3**). The ligand was insoluble in methanol, but its

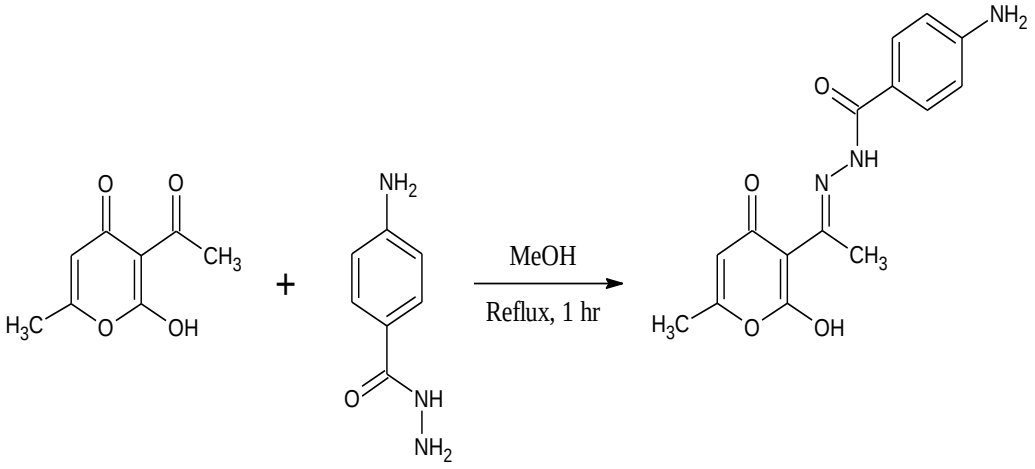

Figure 1. Synthesis of 4-amino-*N*'-[(1*E*)-1-(2-hydroxy-6-methyl-4-oxo-4*H*-pyran-3-yl)ethylidene] benzohydrazide (**HL_1**)

warm suspension reacted with the chloride salts of Cu(II), Zn(II), Ni(II), and Mn(II) to give the complexes (Figure 2). All the synthesized compounds were obtained in good yield (67 – 76 %) and readily soluble in DMSO and ethanol. Unfortunately, no single crystals suitable for X-ray single crystal study were obtained, hence, characterization was reduced to elemental analysis, UV-Vis, FT-IR, ^{1}H NMR, ^{13}C NMR spectroscopy, and mass spectrometry. The results of the elemental analysis (**Table 1**) were in close agreement with the calculated values for the suggested molecular formula. The physical and analytical data of the ligands and complexes are summarised in **Table 1**.

4-amino-N'-[(1E)-1-(2-hydroxy-6-methyl-4-oxo-4H-pyran-3-yl)ethylidene]benzohydrazide (HL_1)

Colour: Lemon green; Yield: 5340 mg, 67%; m.p: 278 °C; Selected IR data (KBr, ν/cm^{-1}): 3466b ν(O-H str), 2915 m, 2849 m ν(aliphatic C-H str), 1635 s ν(C=N), 1275 m ν(C-N str), 1152 m ν(C-O str), 945 m ν(N-N str). ^{1}H NMR (400 MHz, DMSO-d_6): 11.96 (s, 1H, N-H), 7.66 – 6.54 (s, 4H, Ar-H), 5.70 (s, 1H, olefinic), 2.61 (s, 3H, CH_3 pyrone), 2.06 (s, 3H, -N=C– CH_3) ppm. ^{13}C NMR (100 MHz, DMSO-d_6): 181.72 (C_3), 166.64 (C_9), 166.10 (C_5), 163.10 (C_1), 161.43 (C_{13}), 152.00 (C_7), 129.70 ($C_{11,}$ C_{15}), 121.51 (C_4), 113.03 ($C_{12,}$ C_{14}), 107.50 (C_{10}), 94.63 (C_2), 19.60 (C_6), 17.44 (C_8). ESI-MS (*m/z*): (303.14 $[M+H]^+$ 25% , 323.93 $[M+Na]^+$ 69% , 369.92 $[M+ACN+Na]^+$ 100%), Cal. = 301.30. Anal. Calc. for $C_{15}H_{15}O_4N_3$: C, 59.79; H, 5.02; N, 13.95. Found: C, 45.26; H, 4.42; N, 9.53 %; UV-visible (λ_{max}, DMSO, nm): 312 ($\pi\rightarrow\pi^*$), 379, 399($n\rightarrow\pi^*$).

$[Cu(L_1)Cl(H_2O)].H_2O$

Colour: Army green; Yield: 1090mg, 76 %; m.p: 260 °C; Selected IR data (KBr, ν/cm^{-1}): 3445 b ν(O-H str), 3011 w ν(aromatic C-H str), 2923 w, 2849 w ν(aliphatic C-H str), 1747 w ν(C=O str), 1637 s ν(C=N), 1543 s ν(C=C str), 1275 s ν(C-N str), 1181 s ν(C-O str), 1015 w ν(N-N str). ESI-MS (*m/z*): (436.06 $[M]^+$ 17%), Cal. = 435.32. Anal. Calc. For $C_{15}H_{18}O_6N_3ClCu$: C, 41.39; H, 4.17; N, 9.65. Found: C, 39.87; H, 4.45; N, 8.61 %. UV-visible (λ_{max}, DMSO, nm): 261 ($\pi\rightarrow\pi^*$), 371 ($n\rightarrow\pi^*$).

$[Ni(L_1)_2].2H_2O$

Colour: Sea green; Yield: 770 mg, 67 %; m.p: 297 °C; Selected IR data (KBr, ν/cm^{-1}): 3445 b ν(O-H str), 3011 w ν(aromatic C-H str), 2923 w, 2849 w ν(aliphatic C-H str), 1747 w ν(C=O str), 1637 s ν(C=N), 1543 s ν(C=C str), 1275 s ν(C-N str), 1181 s ν(C-O str), 1040 w ν(N-N str). ^{1}H NMR (400 MHz, DMSO-d_6): 8.59 (s, 1H, N-H), 7.54 – 6.17 (s, 4H, Ar-H), 5.82 (s, 1H, olefinic), 2.48 (s, 3H, CH_3 pyrone), 2.06 (s, 3H, -N=C– CH_3) ppm. ESI-MS (*m/z*): (695.28 $[M]^+$ 60% , 717.68 $[M+Na]^+$ 41%), Cal. = 695.30. Anal. Calc. For $C_{30}H_{32}O_{10}N_6Ni$: C, 51.82; H, 4.64; N, 12.09. Found: C, 47.34; H, 4.17; N, 10.40 %. UV-visible (λ_{max}, DMSO, nm): 261 ($\pi\rightarrow\pi^*$), 347 ($n\rightarrow\pi^*$).

$[Zn(L_1)_2].4H_2O$

Colour: Cream; Yield: 930 mg, 76 %; m.p: 263 °C; Selected IR data (KBr, ν/cm^{-1}): 3444 b ν(O-H str), 3011 w ν(aromatic C-H str), 2919 s, 2853 m ν(aliphatic C-H str), 1747 w, 1734 m, 1660 m ν(C=O str), 1646 s ν(C=N), 1532 s ν(C=C str), 1275 s, 1266 s ν(C-N str), 1187 s ν(C-O str), 1011 m ν(N-N str). ^{1}H NMR (400 MHz, DMSO-d_6): 11.30 (s, 1H, N-H), 7.62 – 6.42 (s, 4H, Ar-H), 5.71 (s, 1H, olefinic), 2.48 (s, 3H, CH_3 pyrone), 2.06 (s, 3H, -N=C– CH_3) ppm. ESI-MS (*m/z*): (702.00 $[M]^+$ 42%), Cal. = 702.05. Anal. Calc. For $C_{30}H_{36}O_{12}N_6Zn$: C, 48.82; H, 4.92; N, 11.39. Found: C, 48.87; H, 5.36; N, 10.62 %. UV-visible (λ_{max}, DMSO, nm): 273 ($\pi\rightarrow\pi^*$), 343 ($n\rightarrow\pi^*$).

$[Mn(L_1)_2].4H_2O$

Colour: Yellow; Yield: 850 mg 70%; m.p: 267 °C; Selected IR data (KBr, ν/cm^{-1}): 3434 b ν(O-H str), 2919 s, 2853 m ν(aliphatic C-H str), 1763 w, 1747 w, 1735 m, 1660 m ν(C=O str), 1627 m ν(C=N), 1549 s ν(C=C str), 1266 w, 1232 w ν(C-N str), 1186 s ν(C-O str), 1009 w ν(C-O str). ESI-MS (*m/z*): (708.37 $[M]^+$ 68%), Cal. = 692.55. Anal. Calc. For $C_{30}H_{36}O_{10}N_{12}Mn$: C, 49.52; H, 4.99; N, 11.55. Found: C, 49.70; H, 5.25; N, 10.85 %. UV-visible (λ_{max}, DMSO, nm): 259 ($\pi\rightarrow\pi^*$), 340 ($n\rightarrow\pi^*$).

^{1}H and ^{13}C-NMR Spectra of the Ligands and Complexes

The ^{1}H NMR (**Figure 4**) spectrum of the ligand displayed a weak singlet at 11.96 ppm due to –NH proton. This signal has shifted upfield at 8.59 and 11.30 ppm in the spectra of $Ni(L_1)_2$ (**Figure 5**) and $Zn(L_1)_2$ (**Figure 6**) respectively due to the participation of the adjacent nitrogen atom in coordination. Signals due to aromatic protons were observed within the range 6.17-7.66 ppm in the spectra of the ligand and the complexes. A sharp singlet at 5.70 ppm in the spectrum of the ligand assigned to the olefinic proton of DHA ring has slightly shifted downfield in the complexes. The CH_3–C=N and –CH_3 protons appeared as sharp singlets at 2.06 and 2.61 ppm respectively in the ligand. The ^{13}C NMR spectrum (**Figure 7**) of the ligand showed significant signals that were in good agreement with the build-up of the ligand. The carbonyl carbon of the secondary amide (C_9) and the pyrone ring (C_3) gave signals at 166.64 and 170.24 ppm respectively. The azomethine carbon of the ligand gave signal at 153.95 ppm. In the spectra of $HL_{1,}$ the phenyl carbon nuclei appeared in the region between 113.03–129.70 ppm and pyran ring carbons C_1, C_2, C_4 and C_5 are characterized at 163.10, 94.63, 121.51 and 166.10 ppm respectively. The upfield signals observed in the range 17.44–19.60 ppm were assigned to methyl groups. All these signals shifted downfield in the spectra (**Figure 8**) of the complexes which supported the formation of the complexes.

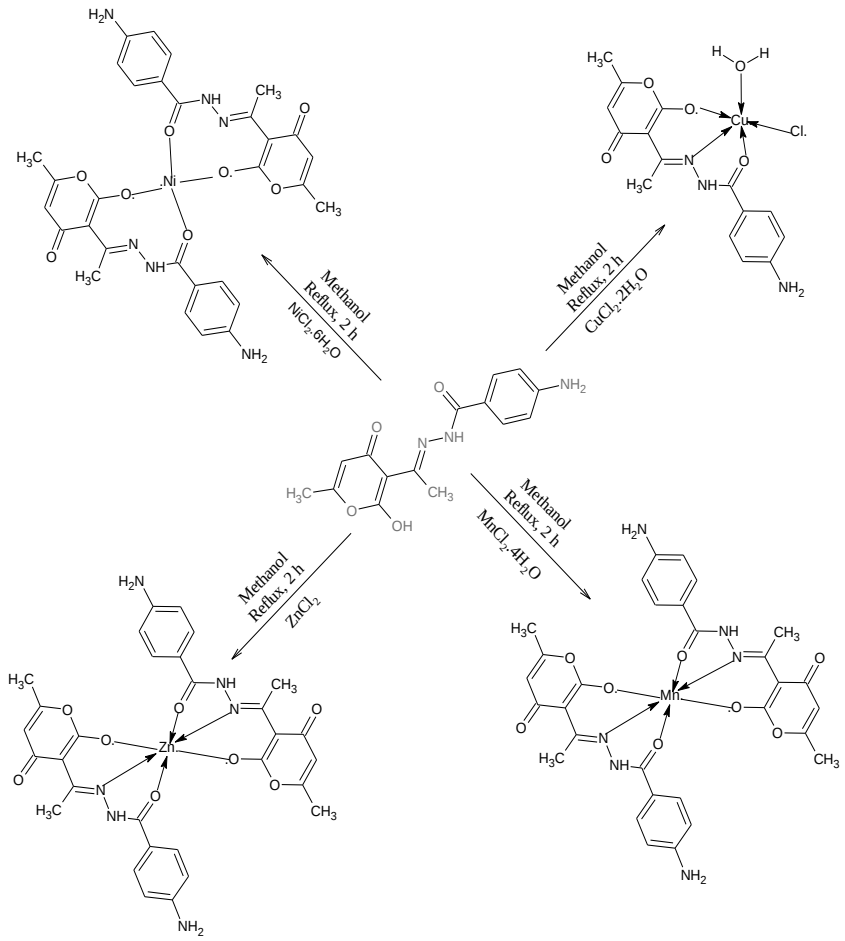

Figure 2. Synthetic route for the preparation of HL_1 complexes

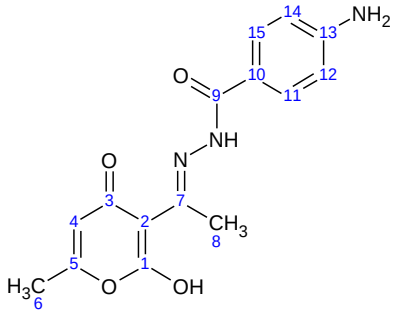

Figure 3. Carbon atom numbering of 4-amino-*N*'-[(1*E*)-1-(2-hydroxy-6-methyl-4-oxo-4*H*-pyran-3-yl)ethylidene]benzohydrazide (**HL_1**)

Table 1. Physical and analytical data of the ligand and its metal complexes

Compound	Molecular Formula	Molecular Weight (g/mol)	Elemental Analysis, % Found(Calculated) C	H	N	Colour	Melting Point (°C)	% Yield
HL_1	$C_{15}H_{15}N_3O_4$	301.30	45.26 (59.79)	4.42 (5.02)	9.53 (13.95)	Lemon green	278	67
$[Cu(L_1)Cl(H_2O)].H_2O$	$C_{15}H_{18}N_3O_6ClCu$	435.32	39.87 (41.39)	4.45 (4.17)	8.61 (9.65)	Army green	260	76
$[Ni(L_1)_2].2H_2O$	$C_{30}H_{32}N_6O_{10}ClNi$	695.30	47.34 (51.82)	4.17 (4.64)	10.40 (12.09)	Sea green	297	67
$[Zn(L_1)_2].4H_2O$	$C_{30}H_{36}N_6O_{12}Zn$	738.05	48.87 (48.82)	5.36 (4.92)	10.62 (11.39)	Cream	263	76
$[Mn(L_1)_2].4H_2O$	$C_{30}H_{36}N_6O_{12}Mn$	727.58	49.70 (49.52)	5.25 (4.99)	10.85 (11.55)	Yellow	267	70

^{1}H NMR (400 MHz, dmso) δ 11.96 (s, 3H), 7.66 (d, J = 7.4 Hz, 41H), 7.50 (d, J = 8.5 Hz, 7H), 6.54 (d, J = 8.5 Hz, 49H), 5.70 (s, 34H), 5.49 (d, J = 51.3 Hz, 21H), 5.40 – 5.32 (m, 2H), 3.33 (s, 10H), 3.16 (d, J = 1.4 Hz, 11H), 3.01 – 2.93 (m, 1H), 2.75 (d, J = 20.9 Hz, 4H), 2.61 (s, 60H), 2.38 (dt, J = 29.0, 18.4 Hz, 54H), 2.12 (s, 4H), 2.06 (s, 62H), 2.01 – 1.35 (m, 21H), 1.49 (s, 1H), 1.49 (s, 5H), 1.32 (s, 1H), 1.24 (d, J = 25.2 Hz, 14H), 0.82 (d, J = 7.4 Hz, 1H).

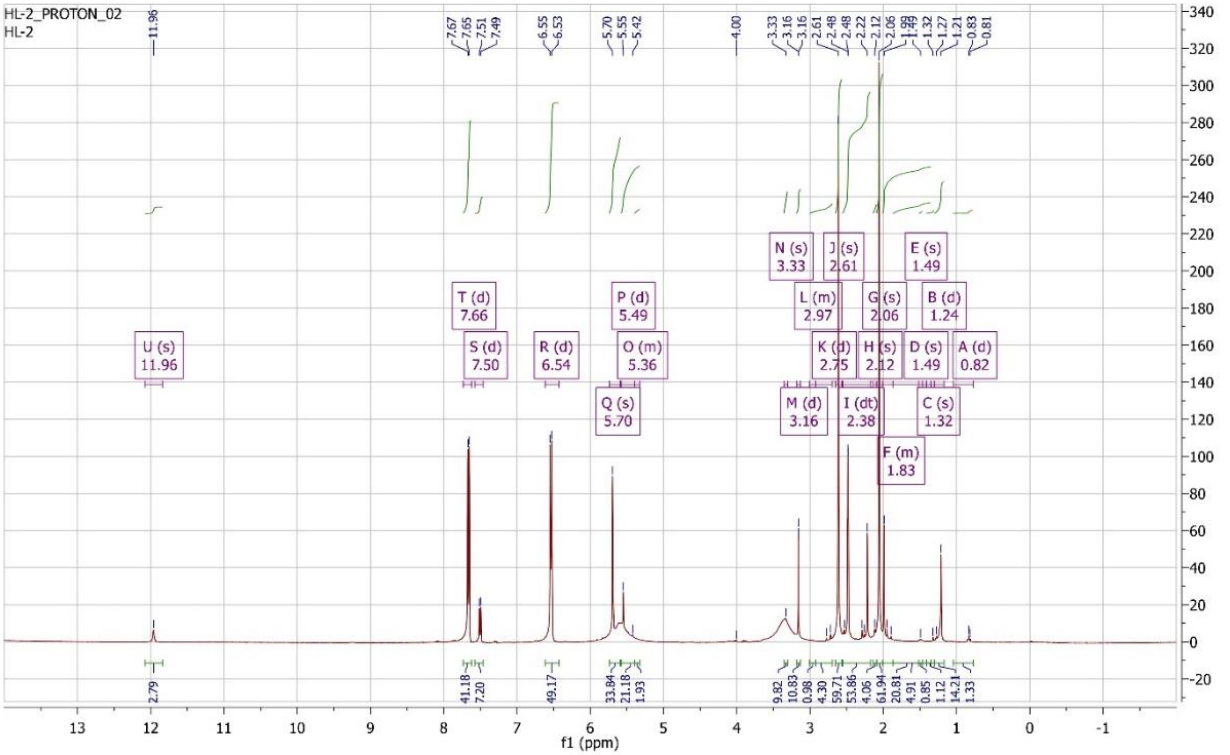

Figure 4: ^{1}H NMR Spectrum of HL_1

^{1}H NMR (400 MHz, dmso) δ 8.59 (s, 138H), 7.54 (s, 3H), 6.54 (s, 18H), 6.17 (d, J = 275.7 Hz, 187H), 3.25 (d, J = 63.9 Hz, 218H), 3.16 – 3.04 (m, 3H), 2.74 (s, 5H), 2.48 (s, 156H), 3.02 – 1.91 (m, 188H), 1.52 (s, 3H), 1.50 (s, 8H), 1.27 (d, J = 42.8 Hz, 48H), 0.83 (s, 4H), -2.05 (s, 145H), -13.10 (s, 3H).

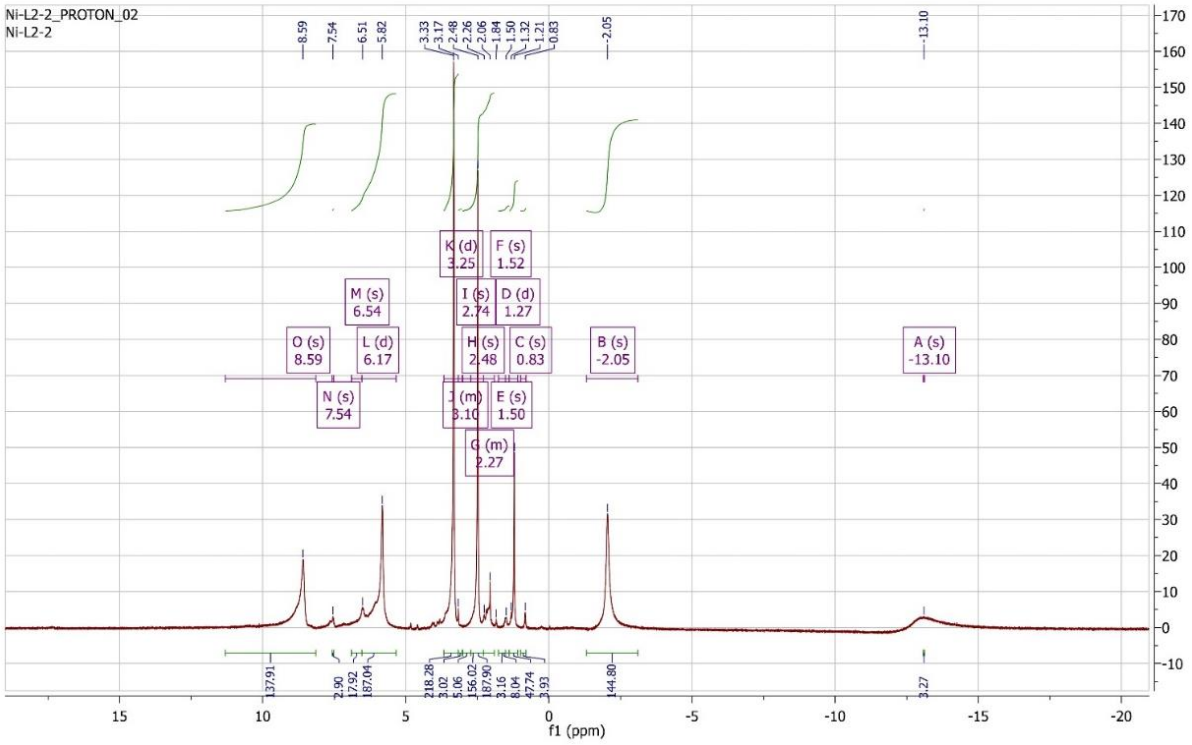

Figure 5: ^{1}H NMR Spectrum of $Ni(L_1)_2$

^{1}H NMR (400 MHz, dmso) δ 7.76 – 7.49 (m, 256H), 6.64 (s, 25H), 6.64 – 6.45 (m, 278H), 6.64 – 5.57 (m, 630H), 4.06 (s, 10H), 3.90 (d, *J* = 6.6 Hz, 7H), 3.73 (d, *J* = 19.6 Hz, 101H), 3.60 (d, *J* = 10.1 Hz, 12H), 3.34 (s, 361H), 3.16 (d, *J* = 3.4 Hz, 50H), 2.60 (s, 69H), 2.58 – 2.40 (m, 292H), 2.36 (s, 40H), 2.25 (t, *J* = 20.7 Hz, 304H), 2.16 (s, 23H), 2.09 (s, 13H), 2.06 (dd, *J* = 10.3, 5.2 Hz, 254H), 2.09 – 1.73 (m, 458H), 1.32 (s, 19H), 1.22 (d, *J* = 7.5 Hz, 95H), 0.82 (d, *J* = 7.1 Hz, 16H).

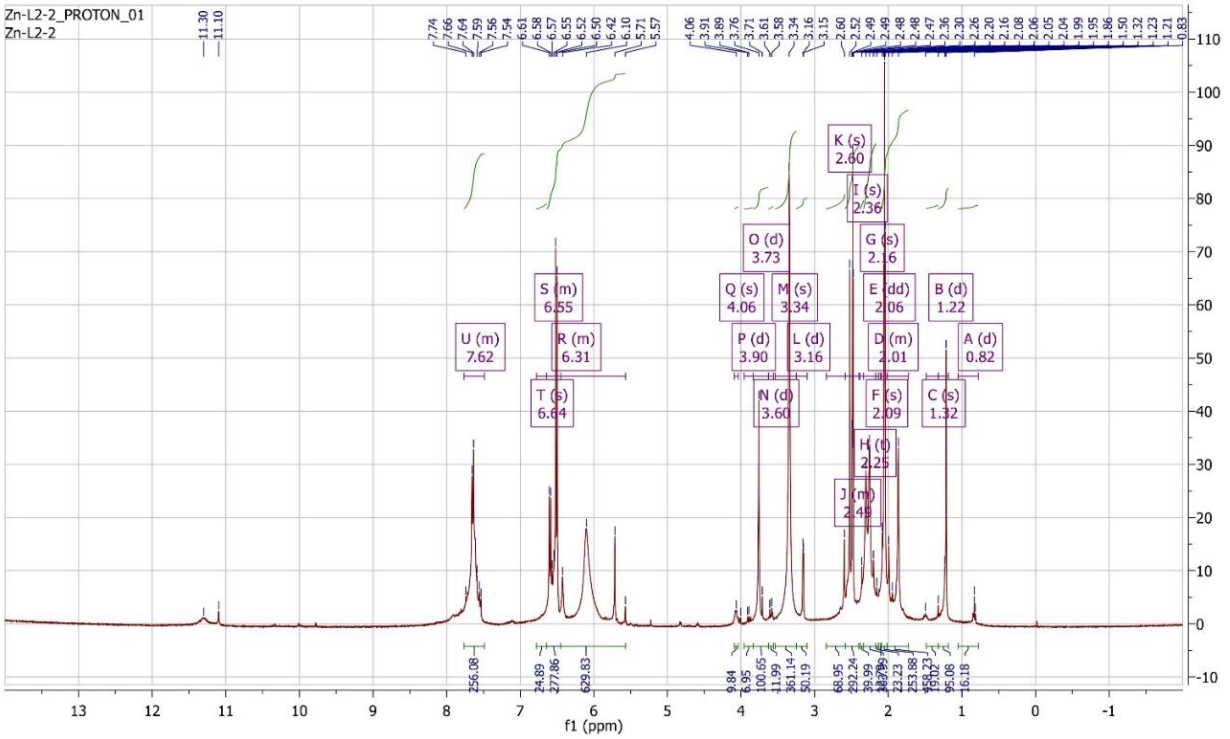

Figure 6: ^{1}H NMR Spectrum of $Zn(L_1)_2$

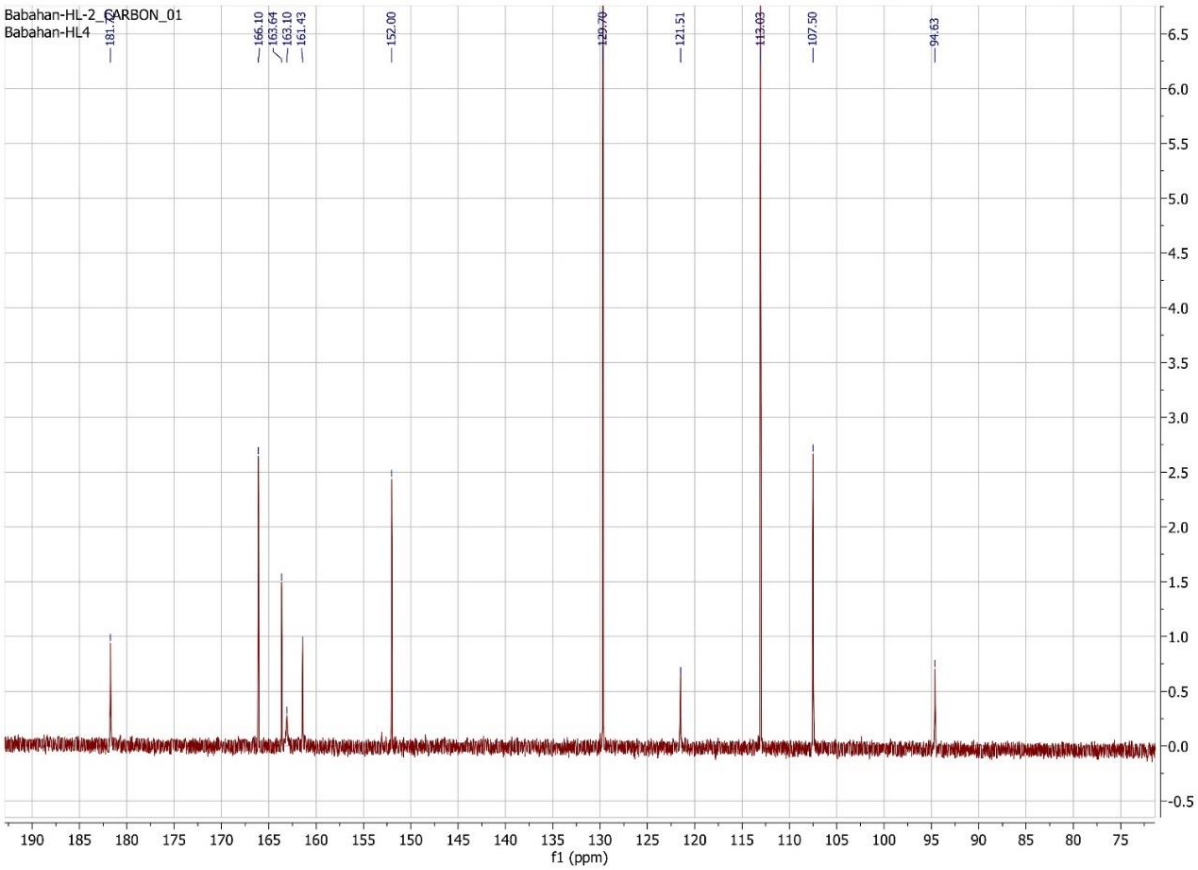

Figure 7: ^{13}C NMR Spectrum of HL_1

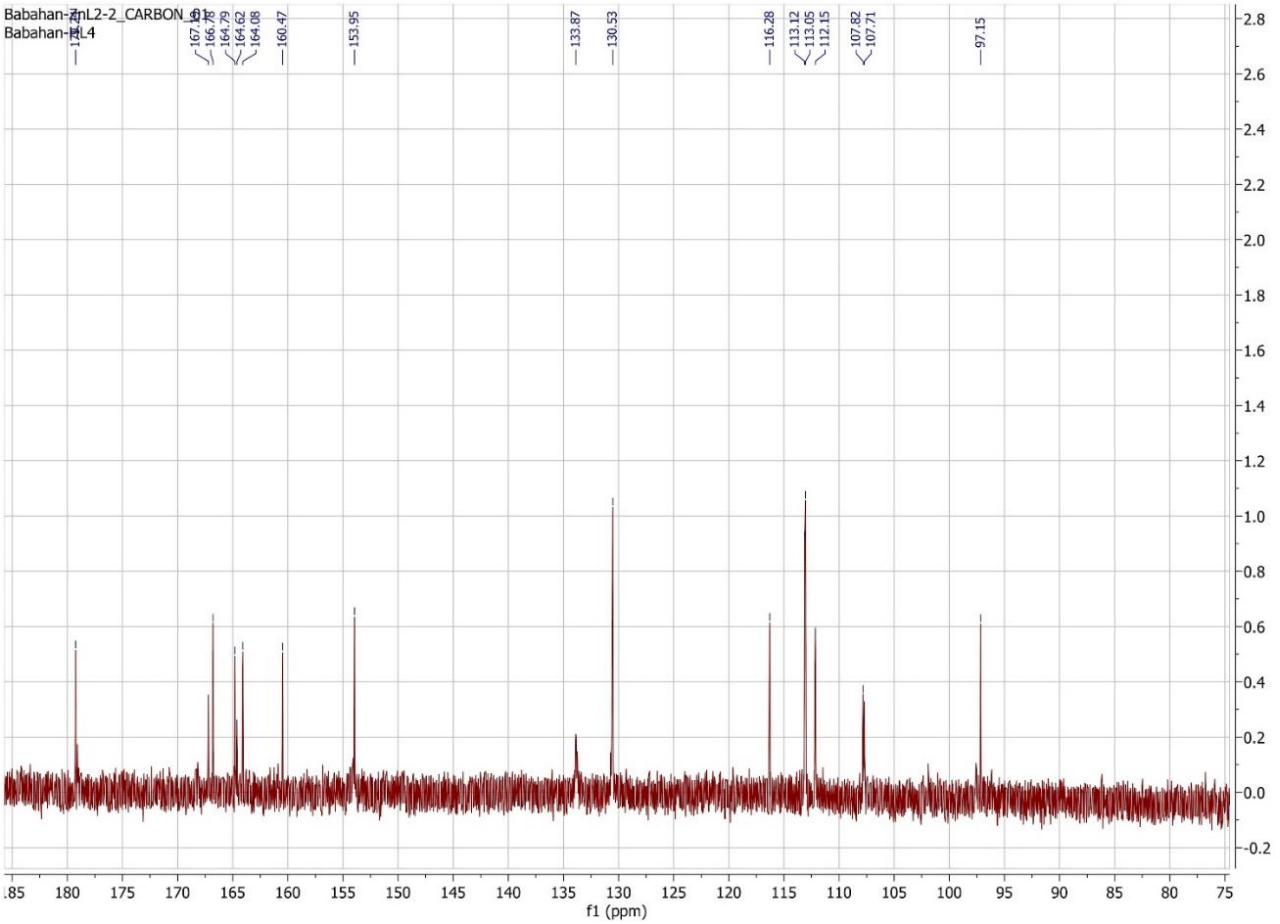

Figure 8: ^{13}C NMR Spectrum of $Zn(L_1)_2$

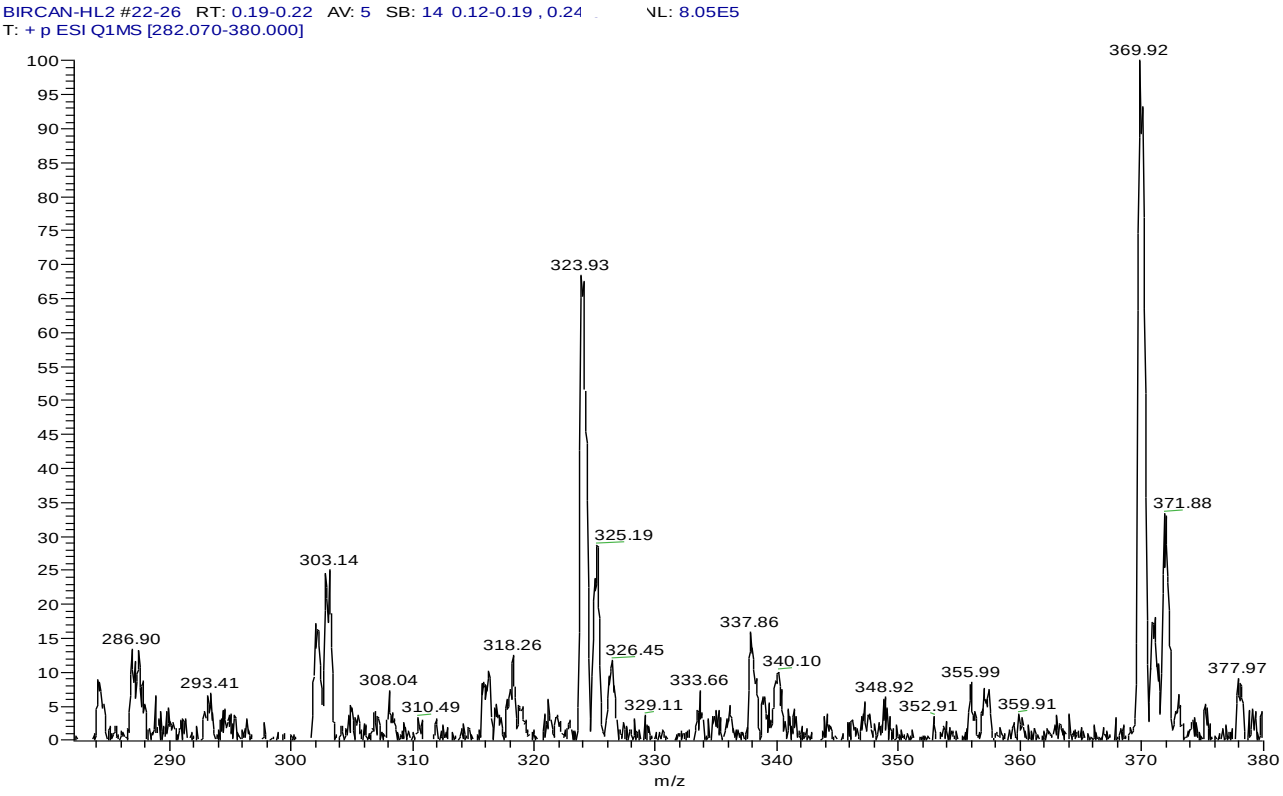

Figure 9: ESI-MS spectrum of HL_1

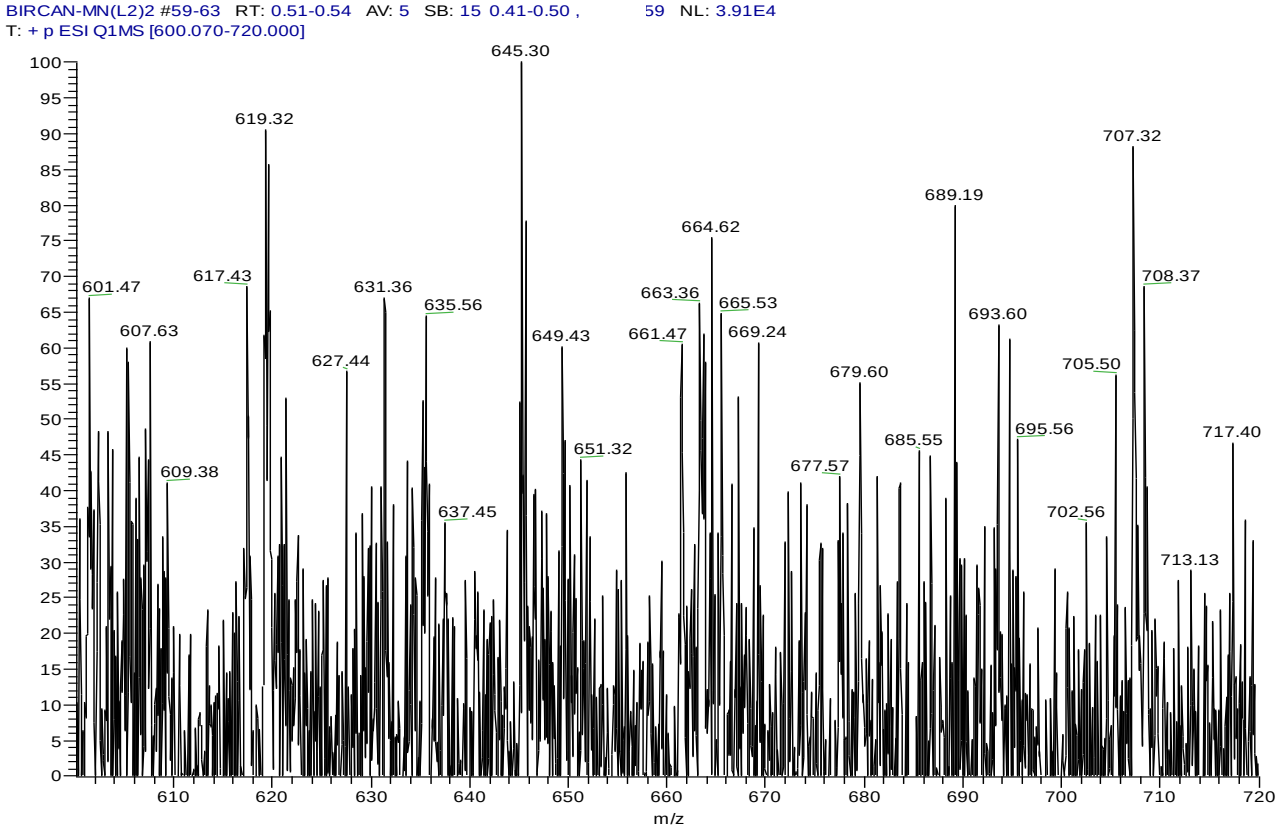

Figure 10: ESI-MS spectrum of $Mn(L_1)_2$

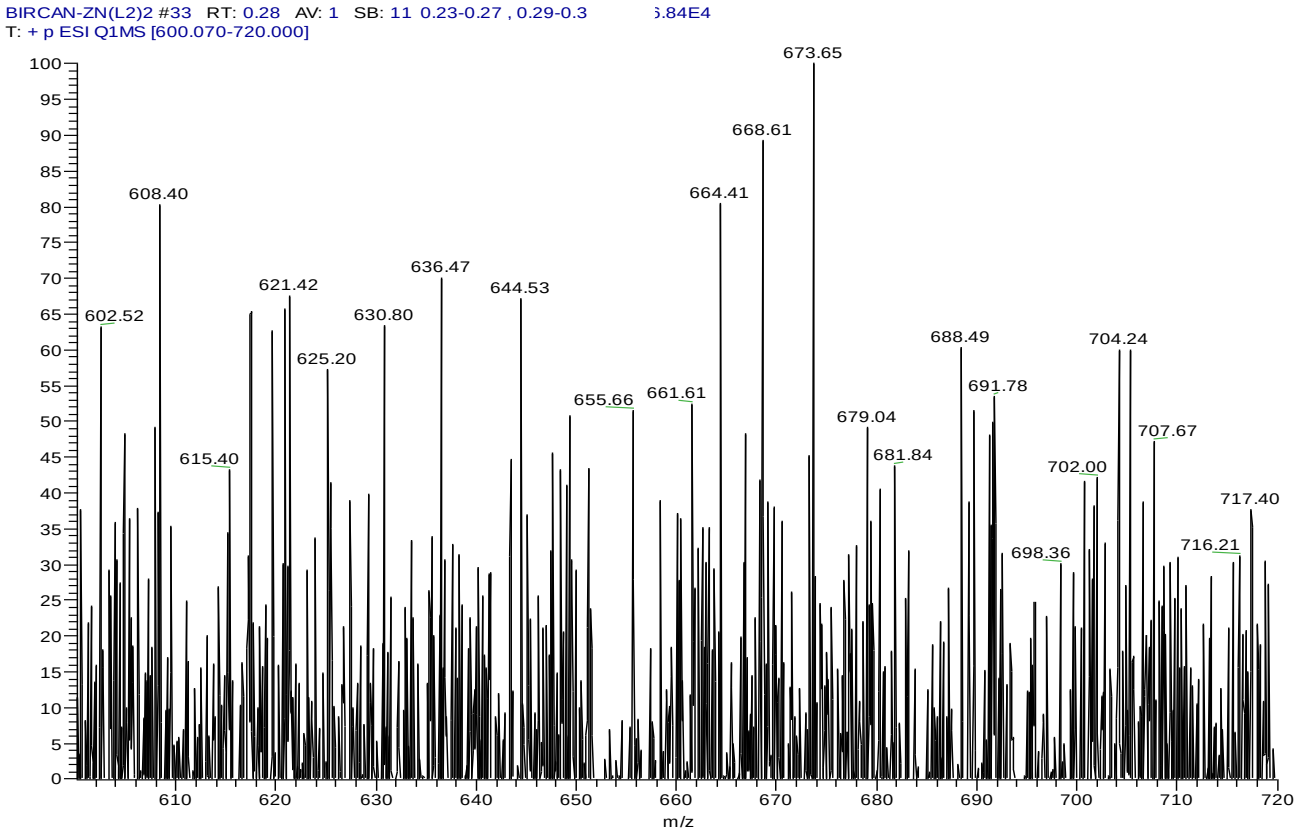

Figure 11: ESI-MS spectrum of $Zn(L_1)_2$

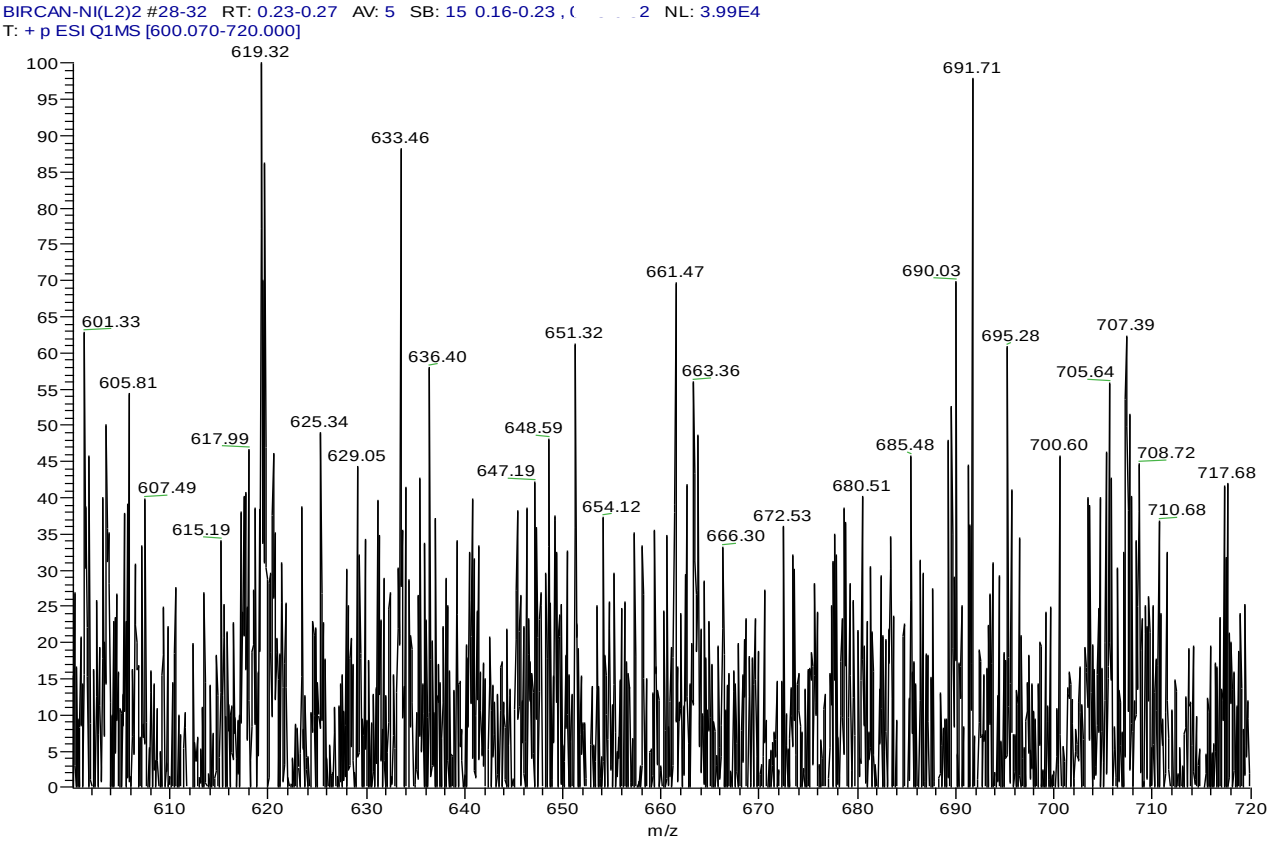

Figure 12: ESI-MS spectrum of $Ni(L_1)_2$\

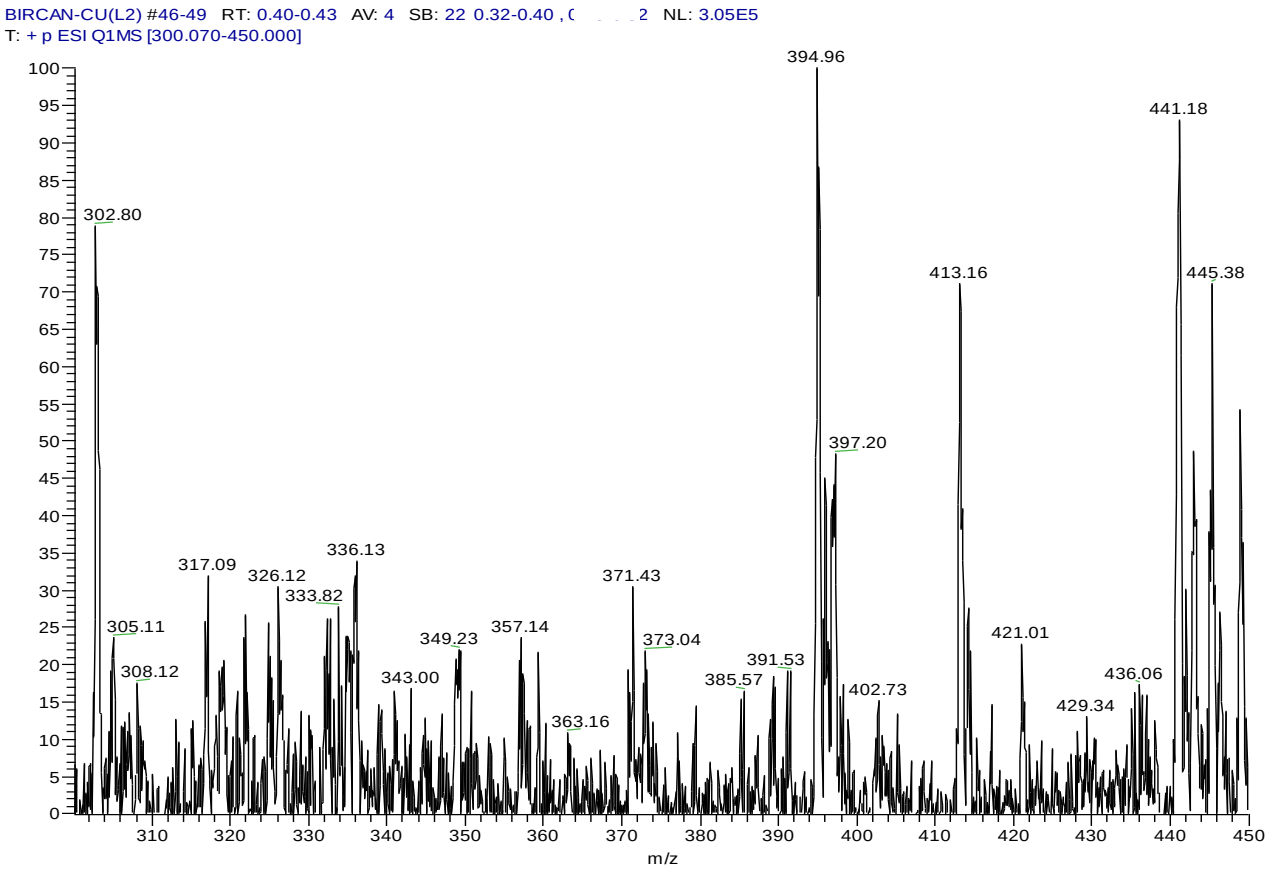

Figure 13: ESI-MS spectrum of $Cu(L_1)$

Mass Spectra and Elemental Analysis

The ESI-MS spectrum (**Figure 9**) of HL_1 has shown the m/z signals at 303.14 and 323.93 for $[M+2H]^{2+}$ and $[M+Na]^+$, respectively, which corresponds to its calculated molecular mass. The peak at m/z 286.90 for the ligand is due to the loss of a methyl group. In the positive mode, ESI-MS spectra (**Figures 10** and **11**) of $Mn(L_1)_2$ and $Zn(L_1)_2$ displayed peaks at m/z 695.56 and 705.48, respectively, corresponding to the loss of a methyl group followed by ammonia. The mass spectrum (**Figure 12**) of $Ni(L_1)_2$ has shown a molecular ion $[M]^+$ peak at m/z 695.28 which was in agreement with its calculated molecular mass. In the spectrum of $Ni(L_1)_2$, the loss of one methyl group is evident by the peak observed at m/z 680.51 and followed by the loss of ammonia evident from the peak at m/z 663.36. The peak observed at m/z 436.06 in the mass spectrum (**Figure 13**) of $Cu(L_1)$ was assigned to $[M+H]^+$ ion. The peaks observed at m/z 607.63 and 617.48 in the spectra $Zn(L_1)_2$ and $Mn(L_1)_2$ respectively were due to the loss of benzoyl fragments suggesting that the C=N bond cleaved easily. Further, the peak at m/z 602.52 in the mass spectrum of $Zn(L_1)_2$ exactly corresponds to $[M]^+$ species of the corresponding ligand. The peak at m/z 302.80 $Cu(L_1)$ is due to $[M+H]^+$ species of the corresponding ligand, thus, confirming the ligand to metal 1:1 stoichiometry. The results of the elemental analysis (**Table 1**) were in good agreement with that of the proposed molecular formula of the ligand and its complexes.

Infrared Spectra of the Ligands and Metal Complexes

The IR spectrum of the ligand HL_1 (**Figure 14**) showed a characteristic broad band at 3466 cm^{-1} which was assigned to ν(O–H) stretching vibration modes. In the IR spectra of the complexes, there was a 10 – 56 cm^{-1} downward shift in ν(O–H) stretching vibrations which suggested the participation of enolic oxygen in coordination with the metal ions. The shifting of the ν(C–O) stretching from 1152 cm^{-1} in the ligand to higher wavenumber 1187 – 1181 cm^{-1} in the spectra of the metal complexes supported the bonding of the enolic oxygen to the metal ions. Also, the IR spectra of the complexes (**Figures 15-18**) showed new bands at ≈3515 – 3911 cm^{-1} due to the OH group of the coordinated water molecules. A band appeared at 1635 cm^{-1} in the ligand due to ν(C=N) stretching modes. This band has shifted to higher wavenumbers in case of the complexes (**Figure 13**) due to the involvement of the nitrogen atom of the azomethine group in coordination to the metal ions (Ekennia et al., 2018). In the IR spectra of the complexes, some new bands due to ν(M–N) and ν(M–O) were observed at 667 – 624 cm^{-1} and 586 – 514 cm^{-1} respectively which supported the formation of Cu(II), Ni(II), Zn(II) and Mn(II) complexes. These bands were absent in the spectrum of the ligand. The band observed 421 cm^{-1} in Cu(II) complex in far-Infrared spectrum of the metal complex was assigned to M−Cl bond suggesting the existence of metal-chloride bond in the Cu(II) complex (Khan et al., 2020). Hence, from the IR spectroscopic data, it has been inferred that the ligand coordinated to the metal ions through the enolic oxygen, amide carbonyl oxygen and azomethine nitrogen atoms.

Electronic Spectra

The UV-Vis absorption spectra of the ligand and its metal complexes are shown in **Figure 19.** The ligand exhibited electronic absorption bands due to $\pi \rightarrow \pi^*$ and n $\rightarrow \pi^*$ transitions, ascribed to the presence of aromatic ring and carbonyl and azomethine functionalities. The ligand showed strong absorption at 312 nm attributed to intra-ligand $\pi \rightarrow \pi^*$ transition. This absorption band has remained almost unchanged in the metal complexes. The n $\rightarrow \pi^*$ transition of the carbonyl and azomethine functionalities was observed between 352 and 377 nm and suffered a blue shift upon complexation, an indication of the coordination of azomethine nitrogen to the metal ions (Al-Shaalan, 2011).

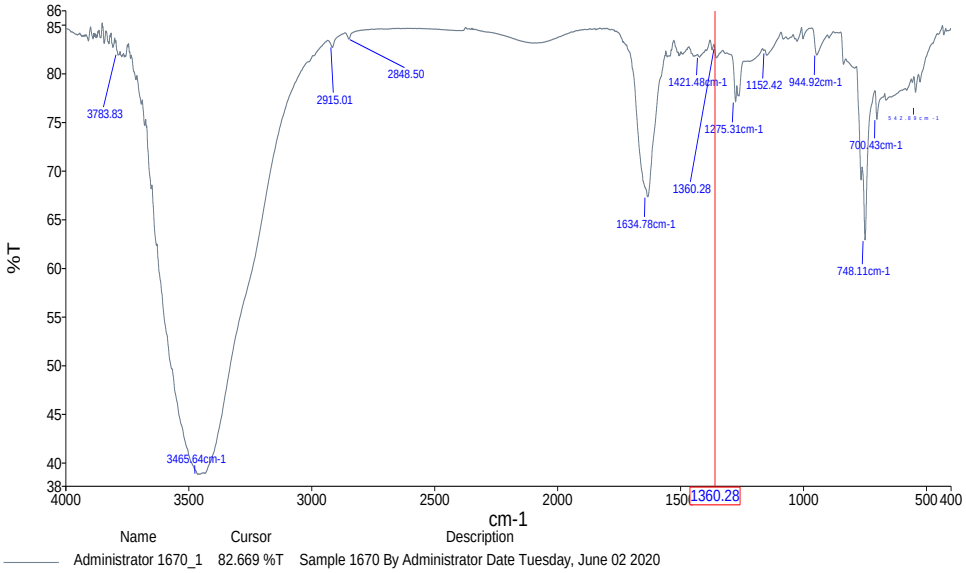

Figure 14: IR spectrum of HL_1

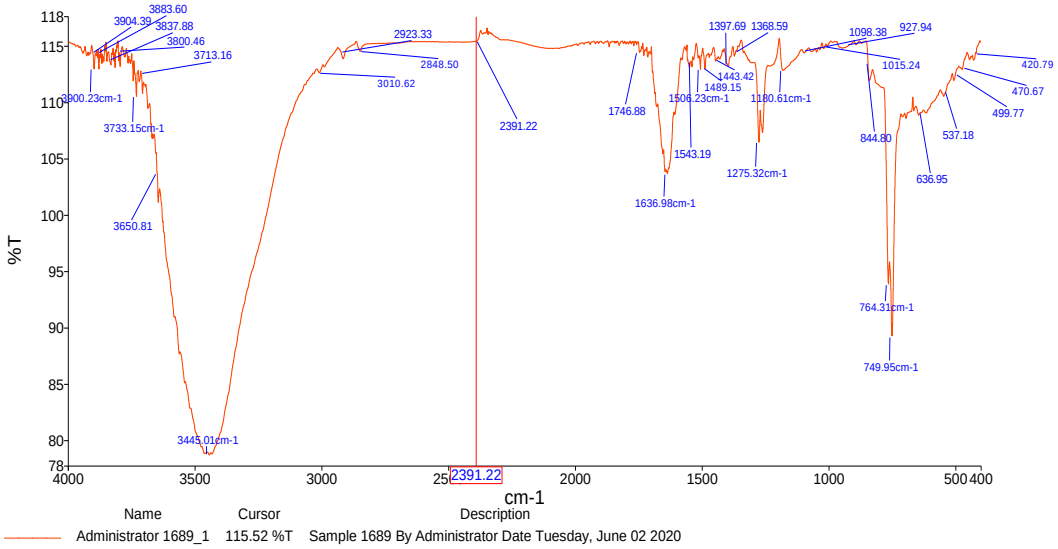

Figure 15: IR spectrum of $Cu(L_1)$

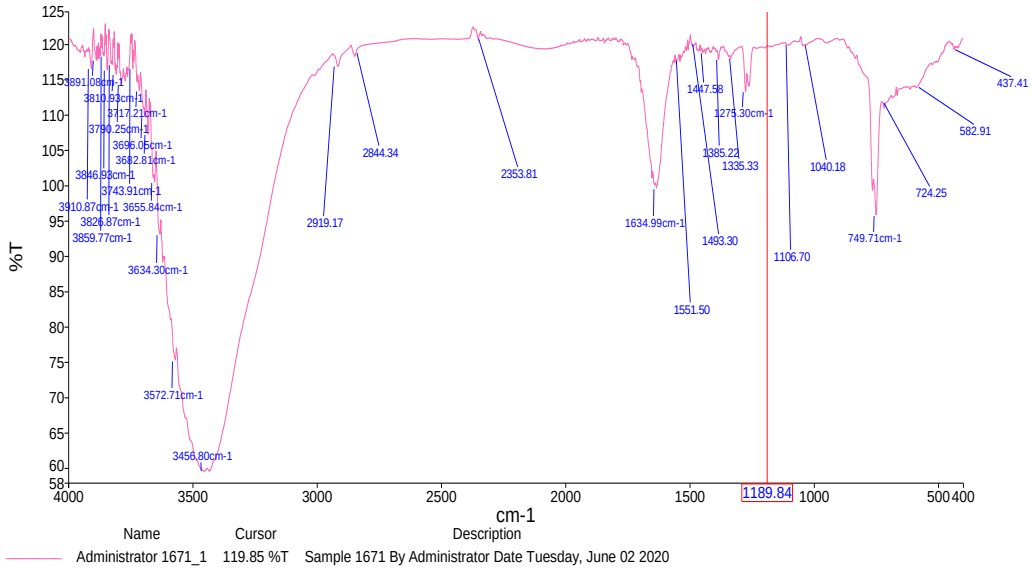

Figure 16: IR spectrum of $Ni(L_1)_2$

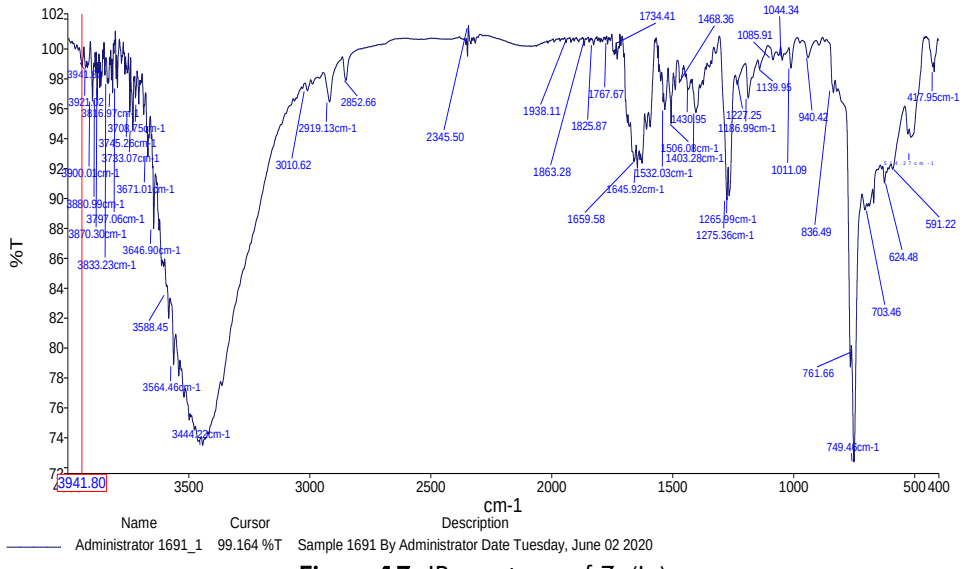

Figure 17: IR spectrum of $Zn(L_1)_2$

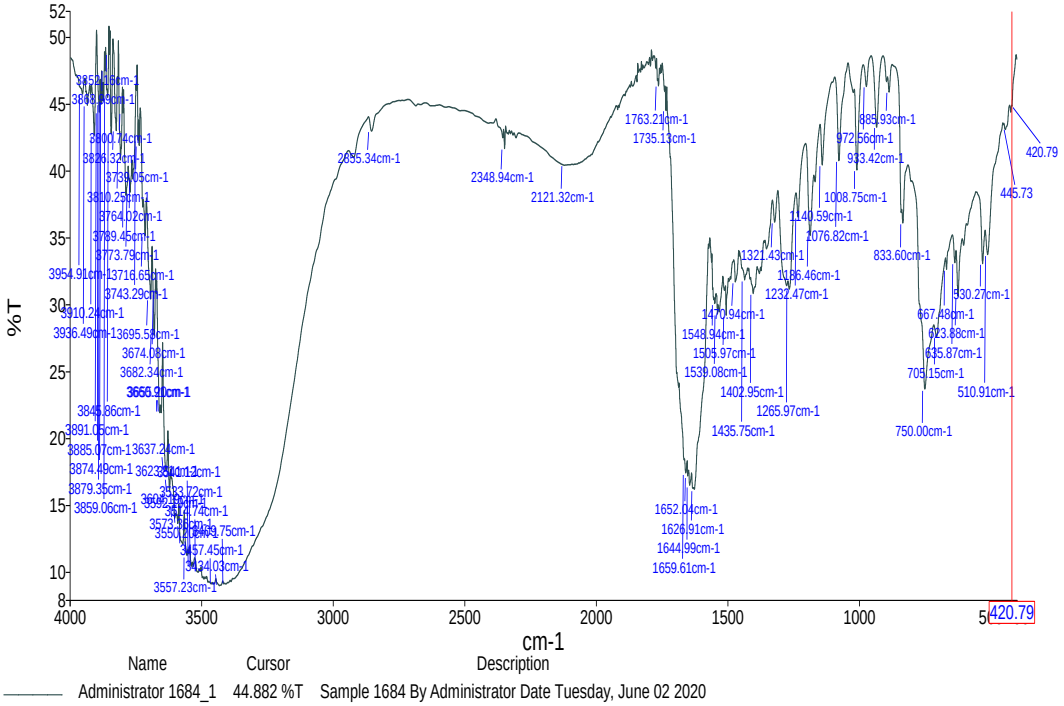

Figure 18: IR spectrum of $Mn(L_1)_2$

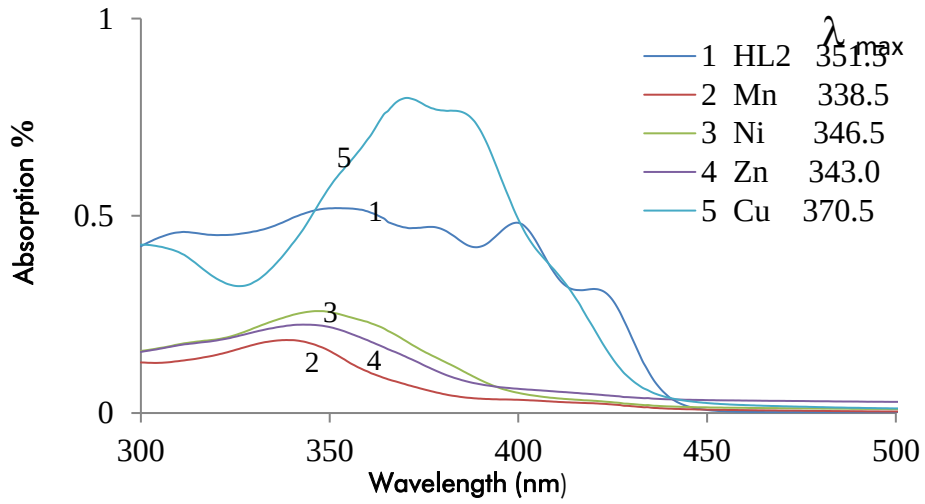

Figure 19. Electronic Spectra of HL_2 and its complexes

CONCLUSIONS

A new benzohydrazone derivative, 4-amino-*N*'-[(1*E*)-1-(2-hydroxy-6-methyl-4-oxo-4*H*-pyran-3-yl)ethylidene]benzohydrazide (HL_1) and its Cu(II), Zn(II), Ni(II) and Mn(II) complexes were synthesized and characterized. According to the analytical and spectral data, HL_1 acts as a monobasic tridentate ligand coordinating to the metal ions through enolic oxygen, azomethine nitrogen and amide carbonyl oxygen except in Ni(II) complex where HL_1 acts as a monobasic bidentate ligand.

CONFLICTS OF INTERESTS

The authors declare that no conflict of interest exists

REFERENCES

Al Alousi, A., Shehata, M.R., Shoukry, M.M., Hassan, S.A., & Mahmoud, N. (2008). Coordination properties of dehydroacetic acid-binary and ternary complexes. *Journal of Coordination Chemistry, 61*(12), 1906–1916.

Al Kubaisi, A., & Ismail, K.Z. (1994). Nickel (II) and palladium (II) chelates of dehydroacetic acid Schiff bases derived from thiosemicarbazide and hydrazinecarbodithioate. *Canadian Journal of Chemistry, 72*, 1785–1788.

Al-Shaalan, N.H. (2011). Synthesis, characterization and biological activities of Cu(II), Co(II), Mn(II), Fe(II), and UO_2(VI) complexes with a new Schiff

base hydrazone: *O*-hydroxyacetophenone-7-chloro-4-quinoline hydrazone. *Molecules*, *16*, 8629–8645.

Arjun, H.A., Elancheran, R., Manikandan, N., Lakshmithendral, K., Ramanathan, M., Bhattacharjee, A., Lokanath, N.K., & Kabilan, S. (2019). Design, synthesis, and biological evaluation of (*E*)-*N*′-((1-chloro-3,4-dihydronaphthalen-2-yl)methylene)benzohydrazide derivatives as anti-prostate cancer agents. *Frontiers in Chemistry, 7*(474), 1–14.

Asif, M., & Husain, A. (2013). Analgesic, anti-inflammatory and antiplatelet profile of hydrazones containing synthetic molecules. *Journal of Applied Chemistry, 2013*(247203), 1–7.

Asyikin, R.A.T., Tay, M.G., & Hashim, H.F. (2017). Synthesis, characterization and antibacterial activities of hydrazone Schiff base compounds and its derivatives. *Malaysian Journal of Analytical Sciences, 21*(5), 1168–1175.

Baldwin, A.G., Bevan, J., Brough, D., Ledder, R., & Freeman, S. (2017). Synthesis and antibacterial activities of enamine derivatives of dehydroacetic acid. *Medicinal Chemistry Research, 27*, 884–889.

Benosmane, N., Boutemeur, B., Hamdi, S.M., & Hamdi, M. (2016). A convenient synthesis of pyrandione derivatives using p-toluenesulfonic acid as catalyst under ultrasound irradiation. *Journal of Fundamental and Applied Sciences, 8*(3), 826–838.

Devi, J., Devi, S., & Kumar, A. (2016). Synthesis, characterization and quantitative structure–activity relationship studies of bioactive dehydroacetic acid and amino ether Schiff base complexes. *Heteroatom Chemistry, 27*, 361–371.

Dutkiewiez, G., Kubicki, M., Narayana, B., Samshuddin, S., & Yathirajan, H.S. (2011). Synthesis of two new Schiff base hydrazones derived from biphenyl-4-carbohydrazide. *Journal of Chemical Crystallography, 41*, 1442–1446.

Ekennia, A.C., Osowole, A.A., Onwudiwe, D.C., Babahan, I., Ibeji, .C.U., Okafor, S.N., & Ujam, O.T. (2018). Synthesis, characterization, molecular docking, biological activity and density functional theory studies of novel 1,4-naphthoquinone derivatives and Pd(II), Ni(II) and Co(II) complexes. *Applied Organometallic Chemistry, 32* (5) e4310.

Fadda, A.A., & Elattar, K.M. (2016). Reactivity of dehydroacetic acid in organic synthesis. *Synthetic Communications*, *46*(1), 1–30.

Gupta, A.K., Pal, R., & Beniwal, V. (2015). Novel dehydroacetic acid based hydrazone schiff's base metal complexes of first transition series: Synthesis and biological evaluation study. *World Journal of Pharmacy and Pharmaceutical Sciences, 4*(1), 990–1008.

Kajal, A., Bala, S., Sharma, N., Kamboj, S., & Saini, V. (2014). Therapeutic potentials of hydrazones as anti-inflammatory agents. *International Journal of Medicinal Chemistry, 2014*, 761030.

Kashar, T.I., & El-Sehli (2013). Synthesis, characterization, antimicrobial and anticancer activity of Zn(II), Pd(II) and Ru(III) complexes of dehydroacetic acid hydrazone. *Journal of Chemical and Pharmaceutical Research, 5*(11), 474–483.

Kendur, U., Chimmalagi, G.H., Patil, S.M., Gudasi, K.B., & Frampton, C.S. (2018). Synthesis, structural characterization and biological evaluation of mononuclear transition metal complexes of zwitterionic dehydroacetic acid *n*-aroylhydrazone ligand. *Applied Organometallic Chemistry, 32*(4), e4278.

Khan, S., Tariqa, M., Ashrafc, M., Abdullahc, S., Al-Rashidad, M., Khalide, M., Taslimif, P., Fatimaa, M., Zafara, R., & Shafiqa, Z. (2020). Probing 2-acetylbenzofuran Hydrazones and their Metal Complexes as α-glucosidase Inhibitors. *Bioorganic Chemistry, 102*, 104082.

Kumar, V. (2018). Hydrazone: A Promising pharmacophore in medicinal chemistry. *Journal of Pharmacognosy and Phytochemistry, 7*(2), 40–43.

Kumar, P., Rai, A., Singh, M., Kumar, D., Sahdev, A.K., & Raj, V. (2016). Review on the pharmacological activities of hydrazone derivatives. *EC Pharmaceutical Sciences, 2*(3), 278–306.

Kurup, M.R.P., Seena, E.B., & Kuriakose, M. (2010). Synthesis, spectral and structural studies of oxovanadium (IV/V) complexes derived from 2-hydroxyacetophenone-3-hydroxy-2-naphthoylhydrazone: Polymorphs of oxovanadium(V) complex [VOL(OCH_3]. *Structural Chemistry, 21*, 599–605.

Liu, L., Alam, M.S., & Lee, D. (2012). Synthesis, antioxidant activity and fluorescence properties of novel europium complexes with (*E*)-2- or 4-hydroxy-*N*'-[(2-hydroxynaphthalen-1-yl)methylene]benzohydrazide Schiff base. *Bulletin-Korean Chemical Society, 33*(10), 3361–3367.

Mangamamba, T., Ganorkar, M.C., & Swarnabala, G. (2014). Characterization of complexes synthesized using Schiff base ligands and their screening for toxicity two fungal and one bacterial species on rice pathogens. *International Journal of Inorganic Chemistry, 2014*, 736538.

Munde, A.S., Jagdale, A.N., Jadhav, S.M., & Chondhekar, T.K. (2010). Synthesis, characterization and thermal study of some

transition metal complexes of an asymmetrical tetradentate Schiff base ligand. *Journal of the Serbian Chemical Society, 75*(3), 349–359.

Okagu, O.D., Ugwu, K.C., Ibeji, C.U., Ekennia, A.C., Okpareke, O.C., Ezeorah, C.J., Anarado, C.J.O., Babahan, I., Coban, B., Yildiz, U., Cömert, F., & Ujam, O.T. (2019). Synthesis and characterization of Cu(II), Co(II) and Ni(II) complexes of a benzohydrazone derivative: spectroscopic, DFT, antipathogenic and DNA binding studies. *journal of molecular structure, 1183*, 107–117.

Oukacha-Hikem, D., Makhloufi-Chebli, M., Amar, A., Bouherrou, H., Rachedi, Y., Meghezzi, H., Silva, A.M.S., & Hamdi, M. (2016). New 2-pyrone-based hydrazones: Synthesis, spectral characterisation, UV–visible study and evaluation of the antiradicalar activity. *Synthetic Communications, 47*(6), 590–598.

Pal, R., Kumar, V., Gupta, A.K., & Beniwal, V. (2014). Synthesis, characterization and DNA photocleavage study of a novel dehydroacetic acid based hydrazone schiff's base and its metal complexes. *Medicinal Chemistry Research, 23*, 3327–3335.

Shakdofa, M.M.E., Shtaiwia, M.H., Morsy, N., & Abdel-rassel, T.M.A. (2014). Metal complexes of hydrazones and their biological, analytical and catalytic applications: A Review. *Main Group Chemistry*, *13*, 187–218.

Sherine, H.B., & Veeramanikandan, S. (2017). Design, synthesis, structural elucidation and biological applications of benzohydrazide derivatives. *Der Pharma Chemica*, *9*(18), 44–50.

Ullah, H., Wattoo, F.H., Wattoo, M.H.S., Gulfraz, M., Tirmizi, S.A., Ata, S., & Wadood, A. (2012). Synthesis, spectroscopic characterization and antibacterial activities of three Schiff bases derived from dehydroacetic acid with various substituted anilines. *Turkish Journal of Biochemistry, 37*(4), 386–391.